Dramatic enhancement of double-walled carbon nanotube quality through a one-pot tunable purification method.

Alexandre Desforges, Angélica Vieira Bridi, Joris Kadok, Emmanuel Flahaut, Francois Le Normand, Jérôme Gleize, Christine Bellouard, Jaafar Ghanbaja, B. Vigolo

Dramatic enhancement of double-walled carbon nanotube quality through a one-pot tunable purification method

Alexandre Desforges [a], Angélica Vieira Bridi [a, 1], Joris Kadok [a], Emmanuel Flahaut [b], François Le Normand [c], Jérôme Gleize [d], Christine Bellouard [a], Jaafar Ghanbaja [a], Brigitte Vigolo [a, *]

[a] Institut Jean Lamour, CNRS-Université de Lorraine, UMR N°7198, BP 70239, 54506, Vandœuvre-lès-Nancy, France
[b] CIRIMAT, Université de Toulouse, CNRS, INPT, UPS, UMR CNRS-UPS-INP N°5085, Université Toulouse 3 Paul Sabatier, Bât. CIRIMAT, 118, Route de Narbonne, 31062, Toulouse Cedex 9, France
[c] ICube - Laboratoire des sciences de l'ingénieur, de l'informatique et de l'imagerie (ICube), CNRS-Université de Strasbourg, UMR N°7357, Rue Blaise Pascal CS 90032, 67081, Strasbourg Cedex, France
[d] Laboratoire de Chimie Physique-Approche Multi-échelle de Milieux Complexes-Université de Lorraine, 1 Bd Arago, 57078, Metz, France

A B S T R A C T

The purification process we propose is a one-pot gas-phase treatment; the CNT powder is simply submitted to a chlorine/oxygen atmosphere at around 1000 °C for 2 h. By varying the oxygen content in an excess of chlorine, the conditions were optimized in order to efficiently remove both metal (catalyst) and carbon impurities from DWCNT samples. Even if a high amount of sample is lost under the oxidative conditions used, a selective elimination of the carbon impurities obviously occurs and a metal impurity removal yield of 99% is obtained from thermogravimetry. Based on a multi-technique approach, we show that the purified DWCNTs are of high structural quality without any surface functionalization. This improvement of the wall quality through the chlorine/oxygen action is seen in particular with a division by 15 of the D over G band intensity of the Raman spectra. Among the existing procedures, the advantages of our purification method are indisputably its simplicity, low time-consuming and high efficiency combined with an enhanced quality of the purified CNTs. Such quasi-pure DWCNTs have high interest since they offer a unique opportunity to study the intrinsic properties and effects of the nanotubes themselves.

1. Introduction

Carbon nanotubes (CNTs) possess unique properties and carry an immense hope for future applications in a wide variety of domains [1]. Among CNTs, double walled carbon nanotubes (DWCNTs) that consist of two concentrically nested single-walled nanotubes are a particular class. Such structure makes DWCNTs the simplest system for studying the effects of inter-wall coupling on the physical properties of CNTs [2–4]. Although it is conceptually a type of multi-walled nanotube, DWCNTs show a combination of outstanding properties only usually encountered for SWCNTs. Regarding their chemical properties, selective functionalization of DWCNTs is particularly interesting because it modifies only the outer wall; the properties of the inner-tube being preserved [5]. DWCNTs are consequently particularly interesting as a model material for CNTs in general. However, like other kinds of CNTs, DWCNTs have drawbacks preventing their large scale implementation; purification is one of the most recognized issues in the domain. Both metal-based residues and carbon byproducts have negative and non-controlled effects for academic study and scale-up processes. Purification is a long-term issue not really solved currently [6–8]. Because the metal-based particles are protected by carbon shells, the strength of the chemical treatments (increase in duration, concentration, or temperature) has to be amplified in order to weaken this protecting carbon coating, this induces however unavoidable damaging of the CNT structure. Damaging of CNTs can be minimized by combining several chemical treatments [9–13]. They are based on the use of i) strong oxidants in liquid medium (HNO_3, H_2SO_4 or $KMnO_4$) and/or gas-phase oxidation even

* Corresponding author.
E-mail address: Brigitte.Vigolo@univ-lorraine.fr (B. Vigolo).
[1] Present address: CAPES Foundation, Ministry of Education of Brazil, Brasilia, DF, 70.040-020, Brazil.

in the more recent works [8,14,15], see also review papers [7,12]; ii) halogens [16–18]; iii) microwave assisted methods that enhance the efficiency by reducing the exposure time [19,20], and see for a review paper [21]. For such approach, the operating conditions used for each treatment have to be optimized depending on the CNT type and source. And, they all use at least one liquid-phase treatment which needs afterwards washing, filtration and drying. Besides that, functional groups are often introduced at the CNT surface and an additional step of annealing of the CNTs is then required in order to remove these introduced defects and recover the CNT structure and properties. Such methods are not really satisfying because they are tricky, multi-step, their selectivity is low, they are not versatile and they are highly time-consuming.

Pure gas phase treatments can be preferred but nevertheless they have been poorly studied. They are either based on high temperature annealing [22,23], or assisted by halogen gases [24–29]. The advantages of these gas-phase methods are several, they are simple (one-step), they do not introduce defects in the CNT structure but they fail to remove carbon impurities. In a previous study performed with arc-discharged SWCNTs, we have shown that a thermal treatment under oxygen added to chlorine could increase the stability of SWCNTs and slightly improve the yield of metal removal compared to a pure chlorine-based treatment from 65% to 75%, but this treatment failed in removing carbon impurities [27]. By applying this single step treatment to DWCNTs prepared by CVD, even if a high amount of sample is lost, both metallic and carbon impurities are removed from the DWCNTs without creating neither defects nor functional groups at the surface of the purified DWCNTs. For the first time, we show that it is possible to prepare high-purity and high-quality DWCNTs by using a straightforward one-pot and entirely gas-phase purification method. It is possible to avoid henceforth the multi-step purification procedures that are time-consuming and involve an inescapable strong attack of the CNT walls.

The paper is organized as follows: after some experimental details, the characterization of the raw sample is firstly presented. The removal of the metallic impurity by Cl_2 alone and Cl_2/O_2 will be investigated before the behavior of carbon species under both purification methods. The focus will then be given on the wall quality of the purified DWCNTs. Finally, we summarize our results and discuss the performance of our method in comparison with those reported in the literature.

2. Material and methods

2.1. Raw DWCNT sample

The used DWCNTs were synthesized by catalytic chemical vapor deposition (CCVD) at 1000 °C from a mixture of CH_4 (18 mol%) in H_2 on a Co:Mo MgO catalyst [30]. MgO is eliminated after synthesis as well as most of Co and Mo-based particles but some of them are tightly encapsulated in graphitic shells and represent the main metal impurities in the raw DWCNT samples (r-DWCNT). Disorganized carbon with a morphology close to crumpled graphene is also present in these samples, and is thought to originate from self-decomposition of CH_4 on the MgO catalyst support [8].

2.2. Chemical treatments

The purification treatment mainly consists of heating the DWCNT powder at the desired temperature for 2 h. Two different processes were applied: the raw DWCNT powder (~90 mg) is placed (i) in a stream of chlorine at a flow-rate of 200 mL/min for 2 h, this process is called P_{Cl}; (ii), in an excess of chlorine for the first hour, and oxygen at a controlled flow added to chlorine for the second hour of treatment, the temperature being maintained at 950 °C for the 2 h, this process is named P_{ClO}. The treated samples using P_{Cl} at 900 °C, 950 °C and 1100 °C are referred as PCl-900, PCl-950 and PCl-1100, respectively. For the treatment under Cl_2/O_2 (P_{ClO}), oxygen flow-rates have been chosen with respects to the amount of carbon expected to be removed. At the high temperature used (950 °C), assuming that the combustion of carbon is rapid and complete (the combustion temperature of the raw DWCNT sample is around 500–600 °C, see TGA results), the combustion is expected to simply follow the reaction: $C + O_2 \rightarrow CO_2$.

The samples purified under Cl_2/O_2 are referred as PClO-1, PClO-2 and PClO-3 depending on the content of O_2 in Cl_2. For PClO-1, the flow-rate was chosen to burn 30 wt% (F1) of the carbon of the sample, for PClO-2, oxygen content is expected to burn 100% (F2) of the carbon species and for PClO-3, oxygen is in excess and the oxygen over carbon ratio is here 170% (F3).

For example for F1 (PClO-1), the weighted raw DWCNT powder was 90 mg, the amount of oxygen required for the combustion of 27 mg (30%) of carbon is then: $27.10^{-3}/12 = 2.25.10^{-3}$ mol of O_2 or a volume of 50 mL of O_2. The flow-rate was then fixed at 0.83 mL/min during the second hr of the purification treatment. For PClO-3, the flow rate was equal to 4.7 mL/min. The used operating conditions are close to those used in the previous study [27] for which the oxygen flow ranged from 0.45 to 4.1 mL/min. The experimental set-up used for the purification treatment is shown in Fig. 1. The chlorine gas was produced *in situ* by the reaction between potassium permanganate ($KMnO_4$) and concentrated hydrochloric acid (HCl). The chlorine gas was fed into the system by a nitrogen stream. Empty vials were distributed throughout the installation to avoid any contact that may arise (in case of overpressure or depression) between the various reagents used. Several vials containing chosen compounds were placed along the chlorine stream in order to remove remaining HCl by the saturated solution of NaCl or moisture by $CaCl_2$ and concentrated sulfuric acid. The purified chlorine gas came into contact with the DWCNT sample heated in the furnace at the desired temperature. In powder form, the sample was previously placed in a silica crucible (10 cm long and 1 cm wide) positioned in the center of a silica tube in the furnace. After reaction with the sample, the excess of chlorine was conducted into another column containing $CaCl_2$, in order to prevent the diffusion of moisture from the output of the circuit to the furnace. Finally, several solutions of sodium hydroxide were used to decompose all unreacted chlorine in chloride and hypochlorite ions and neutralize it. For the oxygen/chlorine-based treatments, the oxygen was fed into the system with a fixed flow-rate by means of a valve. After cooling down the sample was ready for analysis.

After being purified under chlorine alone (P_{Cl}), the samples appeared homogeneous; the whole sample was consequently analyzed. On the contrary, after the Cl_2/O_2 procedure, the samples showed two different aspects (visible to the naked eyes) depending on the location in the silica crucible. The part situated at the input of the Cl_2 stream is less dense and some holes are noticeable while the other part appears much more homogeneous. For this reason the samples were separated into two parts and characterized separately. The aspect of the sample was certainly influenced by its reaction with oxygen since the frontier of this aspect change was more and more located far from the input of the oxygen stream in the oven as the oxygen content was increased. “Entrance” or “ent” is mentioned for the part of the sample which was located on the input side of the Cl_2/O_2 flow-rate and “exit” for the part of the sample which was located on the output side of the Cl_2/O_2 flow. With the increasing content of O_2, the position of this change progressively shifted from the entrance to the exit of the flow. It was located after the first 20% of the crucible length for F1, at around 40% of the crucible length for F2 and at around 80% for F3.

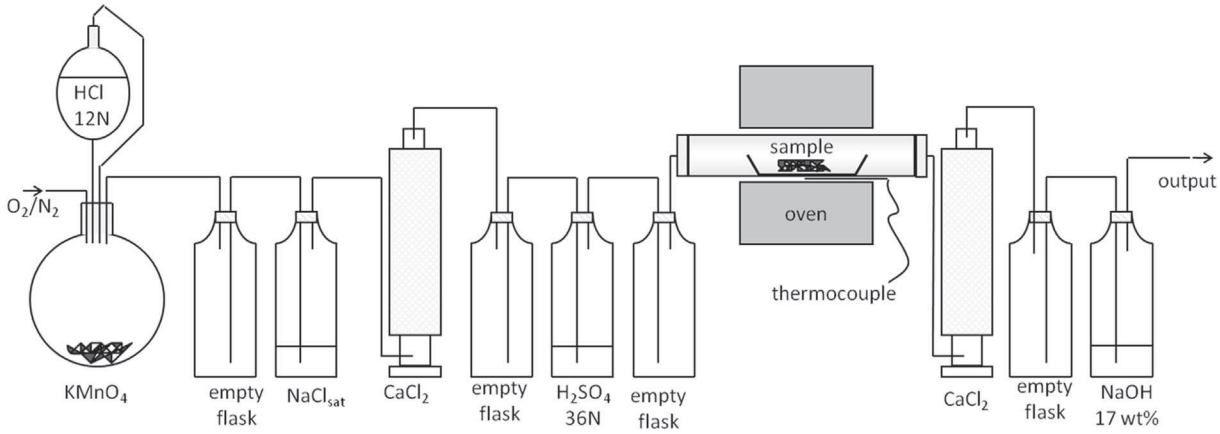

Fig. 1. Experimental set-up used for DWCNT purification with chlorine alone or with a Cl_2/O_2 mixture.

The consumption of the sample, including metal based impurity removal, was estimated from the weight of the powder before and after the submitted chemical treatment. In agreement with the presence or not of oxygen and the oxygen flow-rate, It was around 31 wt% after the PCl process whatever the used temperature and increased to be around 36, 82 and 95 wt% for PClO-1, PClO-2 and PClO-3, respectively. Consequently, it was not possible to collect enough treated DWCNT powder located at the exit for F3 for TGA analysis.

2.3. Characterization techniques

The thermogravimetric analyses (TGA) were performed in a Setaram Setsys evolution 1750 Thermal Gravimetric Analyser. Temperature is increased from room temperature to 900 °C at 5 °C/min under dry air (20 mL/min). The remaining weights correspond to the metallic residues that have been oxidized. The carbon weight losses are determined from the thermograms by the magnitude of the weight lost around the combustion temperature. The derivative curves, dTG, have been normalized to 1; they evidence the ratio between the weight losses at each combustion temperature.

Raman spectra were collected at room temperature (300 K) with a LabRAM HR 800 micro-Raman spectrometer. We have used an incident wavelength of 632.8 nm focused on the samples with a ×50 microscope objective. Typical power densities on the samples' surface were not higher than 0.25 mW/μm^2 in order to avoid over-heating and damaging of the DWCNTs. For analysis, a small amount (around 1 mg) was dispersed in ethanol using a low-power sonication bath (to avoid any introduction of defects) during 5 min. Three spectra were recorded at least on three different zones for the same sample. After subtraction of a baseline, the intensity of the D band over that of the G band, I_D/I_G is calculated for each sample from the maximum intensity of the D and the G band. I_D/I_G is the obtained average values from the recorded data for the same sample and error bars are given in the figure. For comparison of the spectra in the figures, a representative spectrum which I_D/I_G is close to the average value of I_D/I_G of the sample was chosen. The intensity of the spectrum was normalized to the maximum of the G band.

The TEM observations were performed using a Jeol ARM 200F apparatus at an operating voltage of 80 kV, or a JEOL TEM 1400 and 2100 operating at 120 kV. For the observations, raw and treated samples were dispersed in ethanol in a low-power sonication bath for a few minutes and deposited on a holey grid (200 mesh size). Micrographs shown are representative of the 30–40 images taken for each sample. Energy-dispersive X-ray spectroscopy (EDXS) was performed on several zones of the same samples, focusing of nanotube-rich zones, in order to estimate the content of chlorine in the purified samples.

Magnetic measurements have been performed with a SQUID-VSM magnetometer from Quantum Design.

X-ray Photoemission Spectroscopy (XPS) measurements were performed with a monochromatic AlK_α source and a 150 mm hemispherical detector VSW under a base pressure of 5×10^{-9} mbar. Other details about data recording and analysis are reported elsewhere [27].

3. Results and discussion

3.1. The raw DWCNT sample

As for CVD synthesis of SWCNTs, DWCNT formation requires the use of catalysts. These metallic catalysts remain in the sample as an impurity that is widely known to be highly difficult to efficiently remove without damaging the CNTs. In our DWCNT samples, molybdenum and cobalt used as catalyst have been quantified by elemental analysis by Atomic Absorption Spectroscopy to be present at around 1 wt% and 3.5 wt%, respectively [8].

These metal-based impurities were located either close to the DWCNTs in few-layer carbon shells or embedded in large agglomerates of carbon impurities (Fig. 2a and b). These latter due to the self-decomposition of the carbon source (CH_4) on the catalytic support (MgO) contaminate the DWCNT sample. Their quantification can be estimated to be around 30 wt% of the carbon species in the sample. The description and the classification of these carbon impurities are not easy. Especially they seem quite well organized and much more stable than amorphous carbon. These impurities are partly graphitized, as their combustion temperature falls in the same range than that of DWCNTs (Fig. 3). High magnification images evidence the double wall structure of the CNTs, in majority in this sample (Fig. 2c and d). The thermogram of r-DWCNT mainly shows one main combustion temperature around 480 °C (loss of 82 wt %) for which both DWCNTs and the carbon impurities are probably burnt off and a small weight loss is observed around 600 °C (loss of 9 wt%). This could correspond to well organized carbon species like carbon shells which combustion usually falls in this quite high temperature range (Fig. 3), but could also be due to the molybdenum carbide oxidation followed by MoO_3 sublimation, which can occur in a large temperature range starting from 500 °C [31].

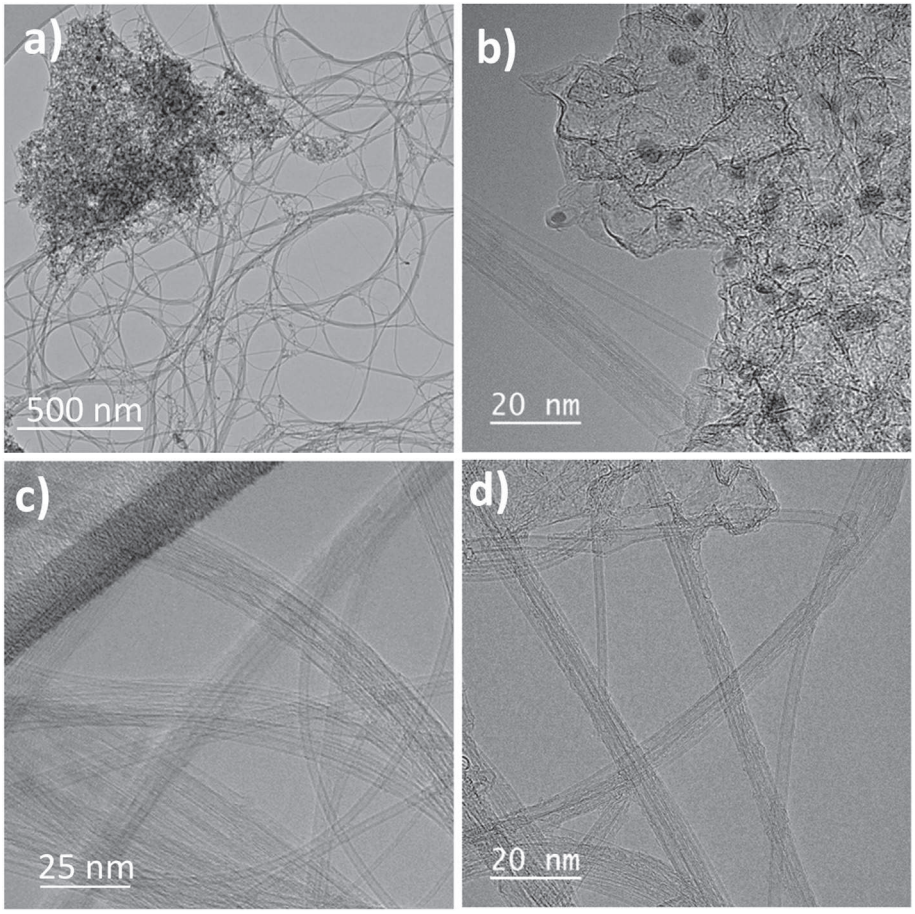

Fig. 2. TEM micrographs of the raw DWCNT sample at different magnifications.

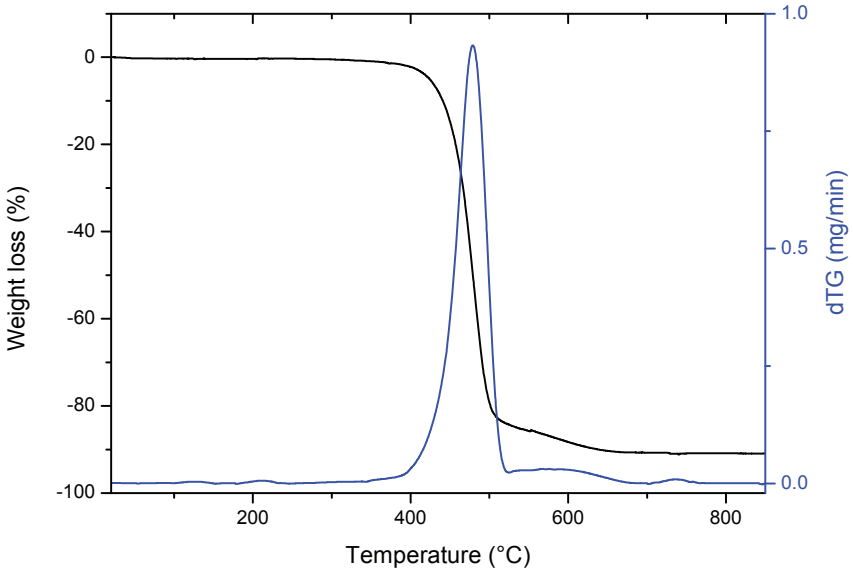

Fig. 3. Thermogram of r-DWCNT and its derivative representation. (A colour version of this figure can be viewed online.)

3.2. Metallic impurity removal using Cl_2 alone

The developed one-pot purification treatment consisting of heating the raw DWCNT powder under a stream of chlorine (P_{Cl}) was applied for 2 h at different temperatures, 900, 950 and 1100 °C.

Thermogravimetric analyses under air have been performed to quantify the amount of metallic residues left after purification. The thermograms obtained for DWCNTs treated under chlorine or

oxygen/chlorine mixture are shown in Figs. 4 and 5, respectively. Table 1 gathers the metal content and the metal removal yield (Y) for the samples being submitted to P_{Cl}. The yield of metal impurity removal is calculated from the residual weight of metal oxides (from the corresponding thermogram at 900 °C) before (RW_b) and after (RW_a) P_{Cl} or P_{ClO} by eq. (1):

$$Y = \frac{RW_b - RW_a}{RW_b} \times 100 \quad (1)$$

Based on TGA results, removal of the metal impurities is significant for all the purified samples (Fig. 4). The content of residual oxides is around 9 wt% for the raw sample and decreases down to around 3 wt% after purification. The efficiency of P_{Cl} is roughly independent of the temperature used for the treatment; the yield of removal being in the 60–70% range for all the purified samples (see also Table 1).

Metal-based impurities in CNT samples are usually difficult to remove with a high yield without damaging or functionalizing the CNT walls. These catalytic residues are indeed either surrounded by thick carbon shells or embedded in carbonaceous impurities. It was especially observed for the raw DWCNT sample used in this work (Fig. 2). In our DWCNT sample, cobalt is under metal form and molybdenum under carbide state [30]. Metal carbides are known to be quite stable against oxidative agents carried out in wet oxidative purification processes. The alternative process we have developed allows high yield elimination of metals, metal oxides and metal carbides [26]. Under our conditions, i.e. a partial pressure of 0.9 atm of chlorine, all these commonly encountered kinds of metal based impurities in CNT samples favorably form metal chloride that is well eliminated by a sublimation-condensation process [28]; the limiting parameter for this chlorine-based process being the accessibility of chlorine to the metal particle and not the chemical reactions themselves.

The P_{Cl} process was shown to successfully remove metallic impurities of both arc discharge and CVD as-produced SWCNTs such as HiPco SWCNTs with high yield (>95% of metal removal [31]). P_{Cl} is obviously less efficient for DWCNTs than for SWCNTs. The proposed main reason for this difference is the quite different nature of the impurities in SWCNT and DWCNT samples. In SWCNTs synthesized by the HiPco method or by arc discharge, metal particles of usually several tens of nm are surrounded by multi-layer carbon

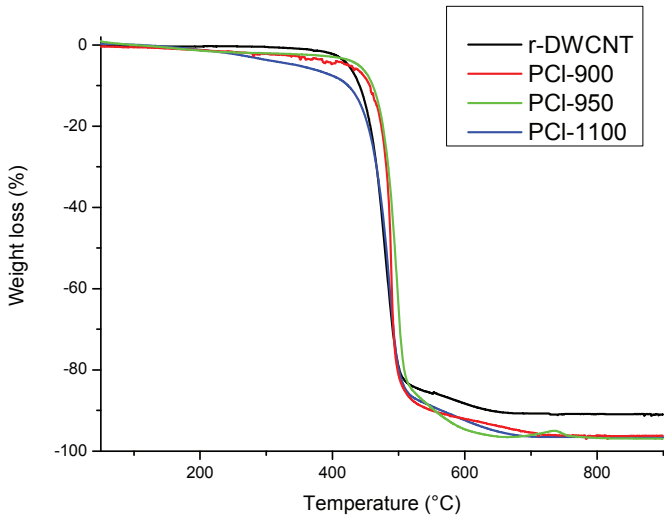

Fig. 4. Thermograms of the raw and the samples purified using P_{Cl} at different temperatures, PCl-900 at 900 °C, PCl-950 at 950 °C and PCl-1100 at 1100 °C. (A colour version of this figure can be viewed online.)

shells. Their facile removal by chlorine was previously explained by a mechanical fracture of the shells due to their dilation after chlorine reaction; metal chloride having lower density than metal, metal oxide or metal carbide usually present at the raw state in the SWCNT samples. The remaining catalyst particles in our DWCNT sample are difficult to observe by TEM because they are quite small (a few nm) and embedded in large carbon impurity aggregates. In these conditions, their accessibility to chlorine is expected to be reduced and the mechanical effect occurring in SWCNT samples is here probably less pronounced.

3.3. *Metallic impurity removal using Cl_2/O_2 mixture*

Oxygen alone or air is commonly used in order to enhance purification of CNTs. It helps in attacking the carbon shield surrounding the protected metal particles. Usually the temperature of treatment under such highly oxidative conditions remains well below the combustion temperature of the CNTs in order to cautiously and gradually attack the carbon and limit the CNT attack. In our treatment (P_{ClO}), oxygen is fed in the reactor containing the DWCNT powder at 950 °C under chlorine keeping the whole process a one-pot treatment.

The shape of the recorded thermograms and combustion temperatures will be discussed in the following section.

By using P_{ClO}, the addition of oxygen leads to an enhancement of the removal yield of the metal-based impurities for the higher oxygen content F3 as deduced from TGA (Fig. 5 and Table 1). For the oxygen flow-rates F1 and F2, except for the sample located at the entrance of the gas flow-rate, the oxygen addition does not affect negatively the efficiency of the metal removal and the removal yield remains in the 60–70% range especially for the samples located at the exit of the oven. From TGA, the yield of purification is dramatically increased and reaches 99% for F3 containing only 0.1 wt% of metal residue which corresponds to 4.10^{-3} at.% of metal impurities. Oxygen is probably able to attack the carbon impurities protecting the metallic particles and improves that way the accessibility of chlorine. Metal chlorides are much more easily formed which is responsible for their good elimination as oxygen is present in chlorine. Furthermore, metal oxychlorides can be also formed due to the presence of oxygen; these latter being also very volatile [32], their formation may improve metal elimination using P_{ClO} compared to P_{Cl}. We point out that such low metallic residue content was not reached by using a similar treatment applied on arc-discharged SWCNTs ([27] and Supporting Information Section 1).

The nature and the estimation of the content of the residual cobalt-based impurities in PClO-3 ent have been investigated by magnetic measurements (see also Supporting Information, Section 2). The results show that the content of cobalt under metal form is as low as 0.01 wt% (the cobalt content in the raw sample is of 3.5 wt %). The amount of metallic cobalt from magnetic measurements in PClO-3-ent is clearly lower than that obtained from TGA (see Supporting Information, Section 3 and Table 1). This discrepancy can be understood thanks to low temperature magnetic measurements showing the presence of a paramagnetic signal attributed to the residual cobalt at an oxidation state of +II (Fig. S2). This Co^{+II} could belong to cobalt chloride ($CoCl_2$) compound remained trapped in the sample. Moreover, the observation of a peak around 9 K in a low field temperature measurement reveals the presence of an ordered $CoCl_2$ intercalated compound, coexisting with paramagnetic Co^{+II} (Fig. S3). The superimposition of these magnetic phases, and the existence of a spin crossover (Fig. S2) prevent any quantification analysis. However, these results show that 99.9% of the Co present in the starting sample has reacted with chlorine to form cobalt chloride. The efficiency of P_{ClO} can be undoubtedly

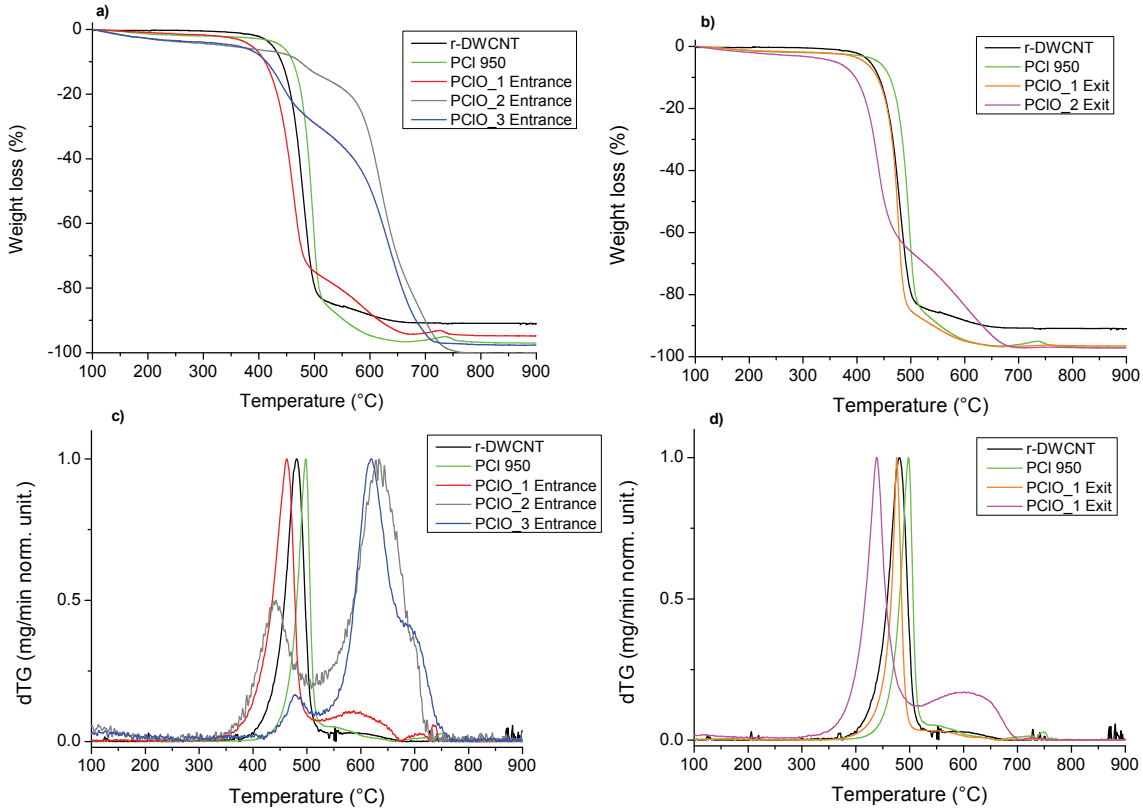

Fig. 5. Thermograms of raw DWCNT, PCl-950 and samples submitted to the P_{ClO} process. a) Samples located at the entrance of the gas flow and b) samples located at the exit of the gas flow. c) and d) being the derivative representation of the weight loss. (A colour version of this figure can be viewed online.)

Table 1
Metal oxide content in the raw and purified samples and corresponding yield of metal impurity removal deduced from TGA.

Sample name	Content of metal oxides (wt%)		Yield (%)	
	Entrance	Exit	Entrance	Exit
Raw DWNT	9.0		–	
PCl 900	3.7		59	
PCl 950	3.0		67	
PCl 1100	3.7		59	
PClO_1	5.4	3.5	40	61
PClO_2	2.5	3.0	72	67
PClO_3	0.1	–	99	–

attributed to the very high reactivity of cobalt with chlorine under the used conditions. Cobalt particles that remained embedded in carbon impurities/shells become accessible with the help of oxygen.

3.4. Behavior of the carbon species under Cl_2 and Cl_2/O_2

The combustion temperature determined from TGA investigation was also analyzed because it allows to compare the stability of each sample against combustion, which can be related to the structural quality of the carbon species.

After the P_{Cl} treatment, all samples show a similar behavior regarding their combustion under dry air (Fig. 3); their combustion begins at around 400 °C and the main combustion temperature is around 480 °C (T1). The combustion temperature was not highly changed after purification using P_{Cl}. There is a small upshift of ~10 °C, which could also be due to the smaller amount of metal available to catalyze the combustion. Another weight loss of weak intensity is visible around 600 °C (T2). It is not possible to assign this high temperature combustion to well graphitized carbon impurities or DWCNTs. Their content of only 5–10% is very low before and after P_{Cl} (Table 2).

Regarding the aspect and the (relative) content of DWCNTs and carbon species, no significant modifications were noticed by TEM for the 3 samples after P_{Cl} (Fig. 6) compared to the raw sample (Fig. 3). From high magnification images, DWCNT walls do not seem damaged by the treatment. This result is in agreement with previous studies on similar treatment conditions (heating at high temperature under chlorine) applied on HiPco and arc-discharge SWCNTs [24].

Representative TEM images with different magnification of the samples treated using P_{ClO} are shown in Fig. 7. As for P_{Cl}, at high magnification, a careful analysis of numerous TEM images reveals that DWCNTs in all the samples treated with P_{ClO} do not seem to have suffered from any damage due to the applied treatment (Fig. 7b, d, f, h, j and l). Raman spectroscopy investigation results (Section 3.5) will allow giving more details regarding the characterization of the structure of the DWCNTs upon the applied treatment.

Lower magnification TEM images reveal some differences regarding the carbon impurity amount in the samples. In images of PClO-1 (both parts) and the part of PClO-2 situated at the flow exit, the typical aspect of the DWCNT sample is recognized (Fig. 7a, c, g) while for the part of PClO-2 located at flow entrance and PClO-3 (both parts), almost no carbon impurities could be observed (Fig. 7e, i, k). These observations are confirmed by low magnification TEM images (Fig. 8).

While for all the other samples, no obvious modification

Table 2
Combustion temperatures and corresponding contents of carbon species removal.

Sample name	Combustion temperature 1 T1 (°C)		Weight loss by combustion at T1 (wt%)		Combustion temperature 2 T2 (°C)		Weight loss by combustion at T2 (wt%)	
	Entrance	Exit	Entrance	Exit	Entrance	Exit	Entrance	Exit
Raw DWNT	481		80		590		5	
PCl 900	491		81		598		7	
PCl 950	498		81		570		10	
PCl 1100	486		75		585		8	
PClO_1	464	479	72	81	589	560	20	10
PClO_2	435	438	14	55	633	600	64	30
PClO_3	480	–	4	–	617	–	82	–

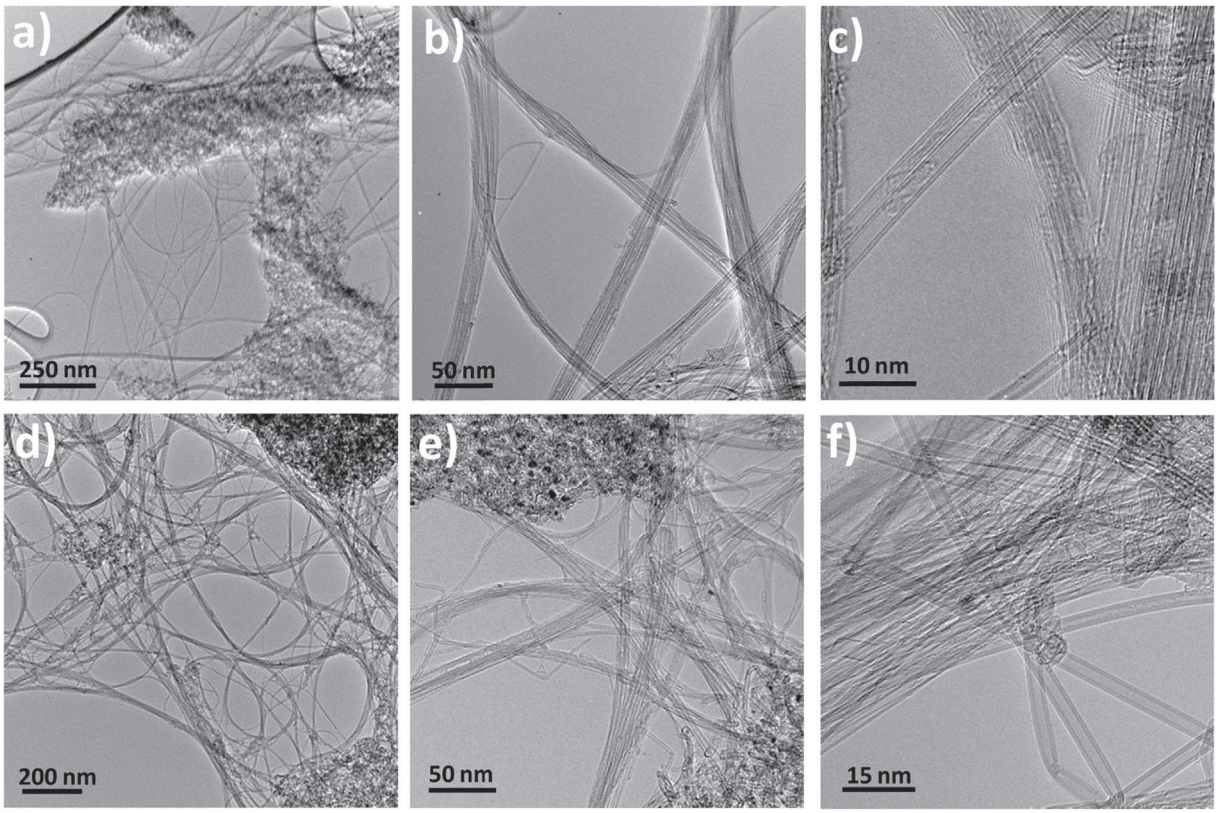

Fig. 6. Typical TEM images of PCl-950 (a, b and c) and PCl-1100 (d, e and f) with different magnifications.

regarding the aspect or the amount of the carbon impurities was noticeable from low magnification TEM observations (Fig. 8), for PClO-2 located at the entrance of the gas in the oven and for PClO-3 (both parts), carbon impurity have almost completely disappeared from the samples (Fig. 8a, c and d). For the sample PClO-2 situated at the exit of the gas stream, carbon impurities have not been removed (Fig. 8b). Even if a significant part of the sample has been lost during the treatment (82 wt% for PClO-2 and 95 wt% for PClO-3), a pseudo-selective combustion of the carbon impurities seemed to occur as the reaction medium was richer in oxygen, either by increasing the used oxygen flow-rate or by the position of the sample in the furnace. The part of the sample located upstream indeed experiences a surrounding medium more rich in oxygen than the part of the sample located downstream since at the set temperature (950 °C) the combustion reaction is expected to be very fast.

From TGA, the main behavior regarding the combustion occurrence of the purified samples was almost unchanged after P_{Cl} and after P_{ClO} for the samples located at the exit of the furnace; they are mainly gasified around 450–500 °C as for the raw DWCNT sample (Table 2 and Figs. 2, 3b and d). For the samples located at the entrance of the oxygen stream, significant modifications related to the content of carbon species burnt off at each mentioned combustion temperature T1 and T2 are observed under oxygen flow-rates F2 and F3 (Table 2 and Fig. 5a and c). The observed behavior seems to be enhanced as the oxygen content is increased in the vicinity of the DWCNT sample; this effect of combustion temperature upshift seems to appear for the sample located at the exit of the furnace for the F2 oxygen flow-rate (Fig. 5d) and it is highly emphasized for the other part of the sample treated under F2 conditions and it is even more pronounced as F3 is used. The recorded combustion temperature upshift is as high as 150 °C.

In the purified samples, the combustion temperature change could be partly attributed to the reduced content of metal impurities after treatment; metal impurities are widely known to act as a catalyst for carbon combustion. Their removal by purification

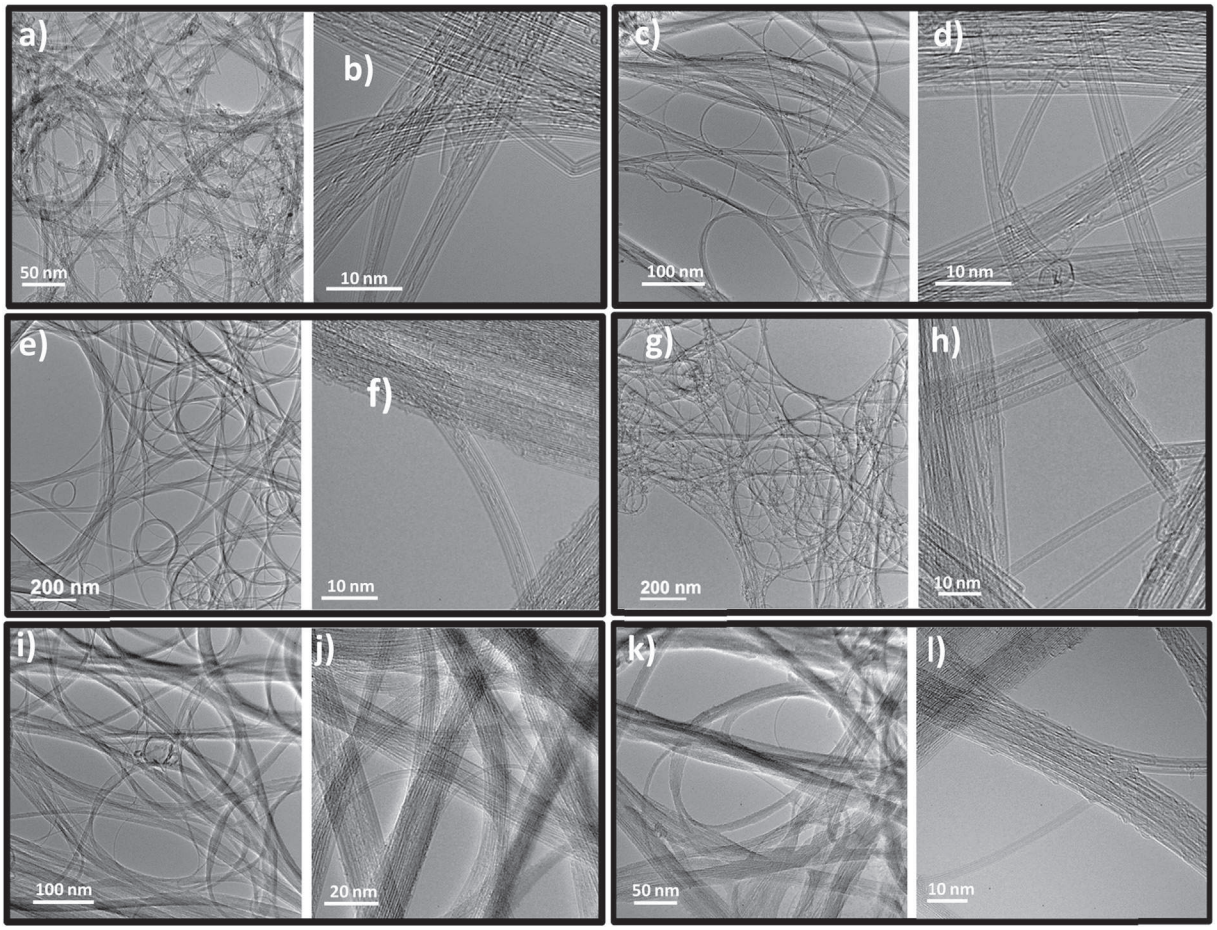

Fig. 7. Typical TEM images with different magnifications of the samples purified using P_{ClO}. PClO-1: a, b, c and d; PClO-2: e, f, g and h; PClO-3: i, j, k and l. Images a, b, e, f, i and j being of samples located at the entrance of the gas stream and images c, d, g, h, k and l being of samples located at the exit of the gas stream.

usually leads to a significant upshift of the combustion temperature especially for samples that contain high amount of metal species such as HiPco SWCNTs for which the raw samples contain more than 35 wt% of iron-based impurities [26]. After purification by a standard or a chlorine-based process, the combustion temperature of purified CNT samples is significantly higher compared to the raw sample, sometimes 100 °C—200 °C or more especially depending on the metal content in the starting sample [33—37] Moreover, here it cannot be the main reason since the amount of metal based impurities is not so high in the raw DWCNT samples and for two samples having close metal-based impurity content, for example in the 2 samples (entrance and exit) treated using P_{ClO} under oxygen flow F2, namely 2.5 and 3.0 wt%, there are more than 150 °C difference between the two combustion temperatures (Table 1); T2 becoming the main combustion temperature for PClO-2 situated at the entrance of the oven. From both TEM and TGA investigations, we attribute this high temperature to the purified DWCNTs that have experienced oxygen-rich atmosphere in chlorine. These highly-purified DWCNTs show a remarkable resistance to oxidation recorded around 600 °C.

3.5. Wall preservation and structural quality of the purified DWCNTs

Raman spectroscopy is a powerful characterization technique for CNTs, including DWCNTs, since the intensity of the D band (around 1350 cm^{-1}) is sensitive to both the structural quality of the CNTs and the presence of carbon impurities in the sample [38—40]. Raman spectroscopy will be useful for studying both (i) the possible damaging that the DWCNT walls could undergo due to the quite aggressive treatment applied (presence of oxygen at temperatures higher than the combustion temperature) and (ii) the efficiency of the carbon impurity removal. The second main feature is the Radial Breathing Modes (RBM) ranging within the 120- 270 cm^{-1} range, typically separated in two forest bands; at low frequency for the outer walls and at a higher Raman shift corresponding to the inner diameter of the DWCNTs. The third feature is the G band (1500-1600 cm^{-1}) corresponding to the tangential vibration modes. The value of the I_D/I_G ratio is usually used to compare the structural quality of the samples. Fig. 9 shows typical spectra of the raw DWCNT sample and after P_{Cl} and P_{ClO} purification process.

Regarding the RBM domain, the Raman spectra of the raw and all the purified samples do not show any strong modifications. The two frequency domains around 150 and 220 cm^{-1} are visible for all the treated samples. That means that the applied purification treatments do not lead to the elimination of a particular population of the DWCNTs that fall in the same range of diameters. The relative intensity of some RBM contributions is however modified. After both P_{Cl} and P_{ClO} treatments, those corresponding to the outer diameters of the DWCNTs, at low frequencies, are more pronounced in the purified samples, in particular for PClO-3-ent. Even if the resonant rules and the coupling effects occurring in such CNT samples, *i.e.* DWCNTs in bundles [41] are not simple to apply, it is possible that the purified DWCNTs were cleaned by either Cl_2 or

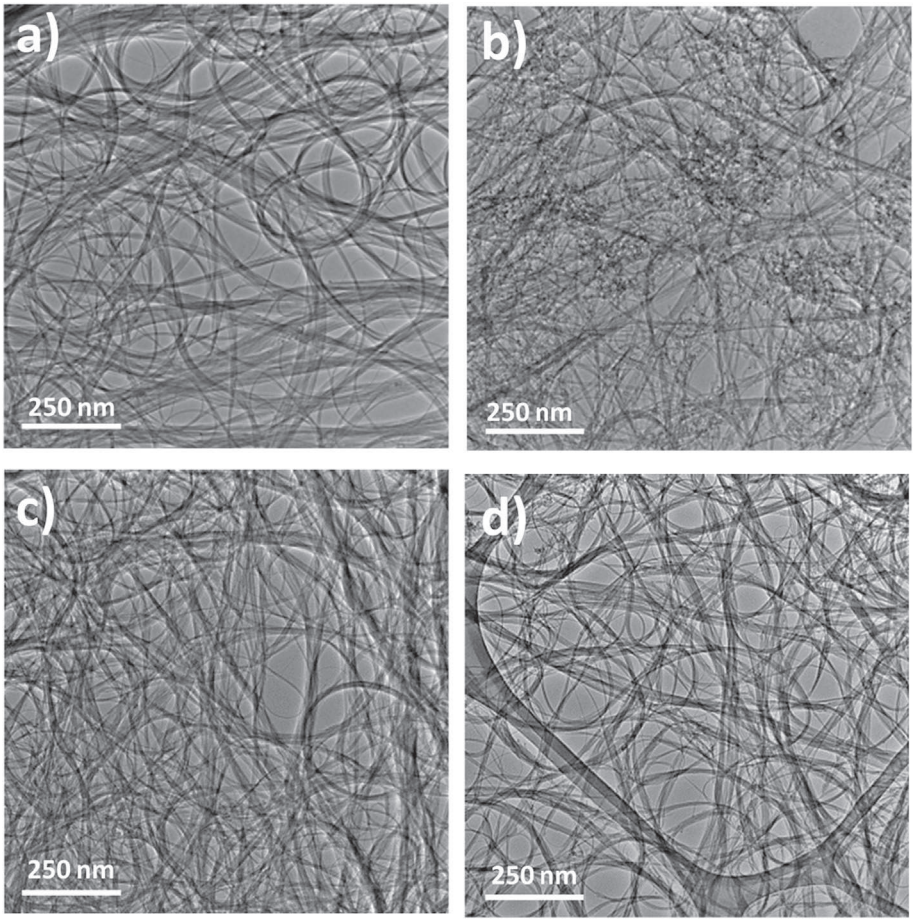

Fig. 8. Typical low magnification TEM images of PClO-2 (a and b) and PClO-3 (c and d) at low magnifications; a and c: samples located at the entrance of the gas stream and b and d: samples located at the exit of the gas stream.

Cl_2/O_2. Carbon impurities that were deposited on the DWCNT surface may be removed enhancing that way the Raman signal from their outer tubes.

Some modifications are noticeable on the D band feature, especially a slight diminishing of the intensity as the temperature of P_{Cl} is increased. After P_{ClO}, the D band is a little bit more pronounced for the oxygen flow-rate F1 and its intensity is highly decreased for F2 and F3 oxygen flow-rates. I_D/I_G ratios for raw and all the treated samples are shown in Fig. 10.

First, I_D/I_G ratio of the raw sample is higher than that recorded for all the treated samples. It is the sign that the DWCNT walls have not been attacked by the treatments. I_D/I_G gradually diminishes from 0.18 for the raw sample to 0.14, 0.11 and 0.07 as the temperature is increased from 900 °C to 1100 °C under chlorine. However only the decrease observed for PCl-1100 can be considered as significant. It is attributed either to removal of a part of the defects of the DWCNT walls or a cleaning effect leading to the removal of a little part of disorganized carbon in the samples due to the high temperature used [42]. Less stable carbon species might be indeed removed by the formation of CCl_4. For the samples purified by the P_{ClO} process with the oxygen flow-rate F1, the sample located at the entrance of the furnace that experiences more oxygen than the part of the sample located at the exit has similar I_D/I_G than the raw sample. For that sample, a lower metal removal yield was also observed (Table 1) as under this low oxygen content condition, DWCNTs were preferentially damaged. For PClO-1-exit, a slight decrease in I_D/I_G is observed compared to that of the raw DWCNTs but it remains quite similar to that of PCl-950 treated at the same temperature without oxygen. I_D/I_G reduction is becoming significant for oxygen flows F2 and F3, being of a factor of 20 for PClO-2-ent, PClO-3-ent and PClO-3-exit. Interestingly, PClO-2-exit shows a different behavior than these three latter samples as it could also be observed by TEM (Fig. 6). This is the reason why this drastic reduction of I_D/I_G can be related to both removal of carbon impurities from the DWCNT samples and elimination of the much more defective DWCNTs. The purified DWCNTs that are able to withstand the highly oxidative conditions used are very clean and of high structural quality. The Raman results are in agreement with the observed combustion temperature upshift observed for the samples PClO-2-ent and PClO-3-ent in which the DWCNTs show an increase of stability against combustion [32,19]. These highly purified DWCNTs have not been attacked and functionalization seems to be avoided by the chlorine/oxygen treatment in agreement with the low content of chlorine in the purified samples found from EDXS and XPS analyses (see Supporting Information, section 4).

3.6. *Purification efficiency*

According to the studies on CNT purification, five aspects are relevant to evaluate the efficiency of a CNT purification method: i) elimination of metal-based impurities (coming from the catalysts), ii) elimination of carbon impurities, iii) preservation/enhancement of CNT quality without functionalizing/damaging their walls, iv) sample/CNT consumption, v) simplicity and time consumption of

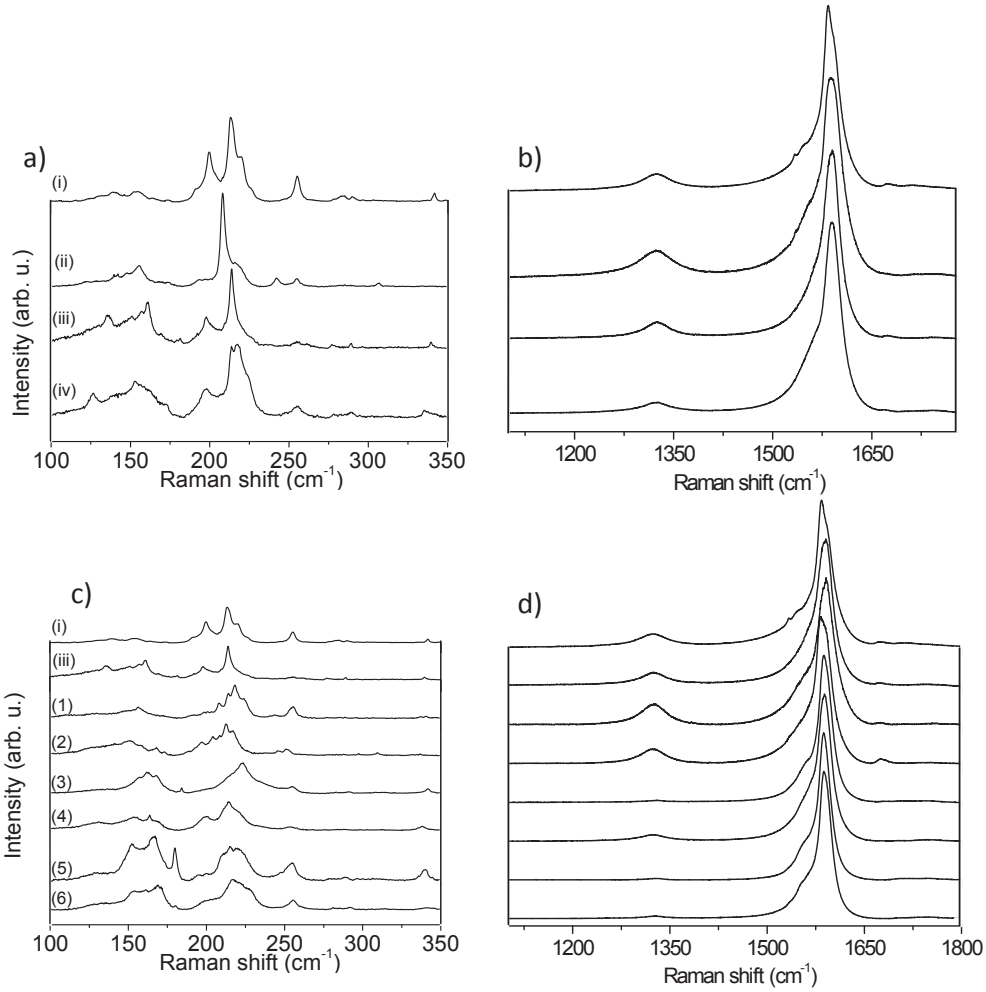

Fig. 9. Raman spectra of the raw and the samples purified using P_{Cl} a) RBM domain; b) D and G band domain and samples purified by P_{ClO} c) RBM domain; d) D and G band domain. (i) raw DWCNT, (ii) PCl-900, (iii) PCl-950, (iv) PCl-1100, (1) PClO-1-ent, (2) PClO-1-exit, (3) PClO-2-ent, (4) PClO-2-exit (5) PClO-3-ent, (6) PClO-3-exit.

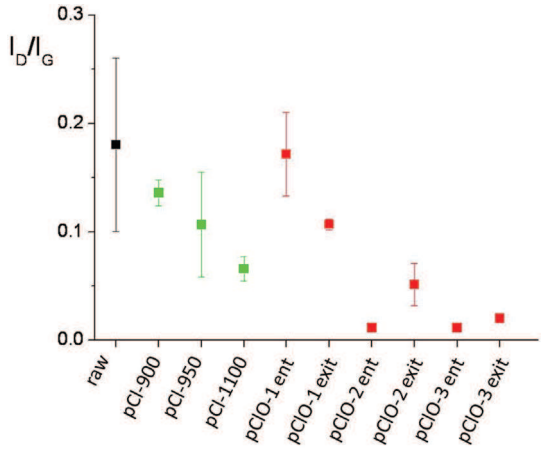

Fig. 10. I_D/I_G ratios for raw and all the treated samples. (A colour version of this figure can be viewed online.)

the method. Table 3 gathers the results obtained from the literature. Among the high number of published papers on the purification of CNTs, the selected papers are those showing high efficiency regarding both metal removal (metal impurity removal yield or Y_m) and structural quality of the purified CNTs and in which the sample consumption (sample yield or Y_s) was reported. For the sake of clarity of the discussion, the papers have been ordered in Table 3 depending on the number of steps of the method (N) which allows to appreciate the criterion v). Preservation of the quality of the purified CNTs is conventionally quantified by I_D/I_G ratio from Raman spectroscopy (I_D/I_G of the raw sample is also reported as reference).

Among the methods with a low number of treatment steps ($N < 3$), excluding the present study, only the treatment reported by Ko et al. [43] allows to remove the carbon impurities by keeping good catalyst removal and sample yield (93 and 75%, respectively). Nevertheless, the CNT quality is rather poor (I_D/I_G 0.15) compared to the other works. An improvement of the CNT quality together with a good carbon impurity elimination (and a good catalyst yield) suffers from multi-step and complex preparation methodologies [13,46]. The number of treatments is indeed often quite high in the reported approaches and they include at least one liquid phase treatment which requires subsequently filtration and washing (often several times with different solvents) and the washed CNTs have also to be carefully dried. Moreover, as expected, standard acid attack or thermal oxidation under air/oxygen inevitably induces a decrease of sample yield [8,45]. Li et al. [46] found an improvement of CNT quality (I_D/I_G decreasing by a factor 2) with a sample yield of only 38% and Sheng et al. [13] could even more enhance the quality

Table 3
Efficiency of various CNT purification methods in comparison with our developed treatment. N is the number of treatments of the purification procedure. In case of liquid phase treatment, a filtration/drying step is necessary to recover usable nanotubes; to take this into account, N is considered strictly superior to the number of chemical treatments. Y_m is the metal impurity removal yield calculated by $100 \times (m_i - m_f)/m_i$ where m_i and m_f are the content of metal impurities in the sample before and after purification, respectively. For each study, only the best yield is reported in the table. Y_s is the sample yield calculated by $100 \times (m_{si} - m_{sf})/m_{si}$ where m_{si} and m_{sf} are the weights of the initial and final sample, respectively.

Ref.	CNT type	Purification method		Carbon impurity elimination	Y_m (wt %)	I_D/I_G of the raw CNTs	I_D/I_G of the purified CNTs	Y_s (%)
		N	Description					
This work	DWCNT	1	Cl_2/O_2 at 950 °C, oxygen flow 2 exit (PClO-2 exit)	No	67	0.18	0.05	25.1
This work	DWCNT	1	Cl_2/O_2 at 950 °C. oxygen flow 2 ent (PClO-2 ent)	Yes	73	0.18	0.012	8.5
[43]	MWCNTs	>1	Microwave in HNO_3	Yes	93.3	N.A.	0.15	75
This work	DWCNT	1	Cl_2/O_2 at 950 °C, oxygen flow 3 ent (PClO-3 ent)	Yes	99	0.18	0.012	4.3
[27]	SWNT arc discharge	>2	Cl_2/O_2 at 950 °C + washing	No	76	1.8	0.5	26
[8]	DWCNT	>2	HNO_3/H_2SO_4 (70 °C)+ washing	No	78	0.2	0.05	18
[8]	DWCNT	>3	Reflux in HNO_3 + HNO_3/H_2SO_4 (70 °C) + washing	No	82	0.2	0.08	16
[18]	SWCNTs	>3	(O_2 + $SF_6/C_2H_2F_4$) + HCl extraction + hexane washing	Yes	50	0.04	0.03	50
[44]	SWCNTs	>4	Reductive method: NaNp/ DMAc + centrifugation + oxidation + washing	N.A.	74	0.031	0.02	74.4
[45]	SWCNTs	>4	HCl (several times) + reflux in HNO_3 + washing	No	88	0.32	0.05	30
[20]	MWCNTs	>4	Microwaves in water ×10	No	94.4	0.2	0.22	88
[46]	SWCNTs	>4	Dispersion in benzene + washing + HCl (ultrasounds) + freezing + washing	Yes	95.4	0.29	0.13	38
[13]	SWCNTs	>4	Ar-H_2 at 800 °C + HCl washing + oxidation in air at 400 °C + washing (×2)	Yes	98.8	0.06	0.013	21.6
[13]	SWCNTs	>4	Oxidation in air at 400 °C + HCl washing + Ar-H_2 at 800 °C + washing (×2)	Yes	99.83	0.06	0.014	12.8

of the purified CNTs with their method (decrease of I_D/I_G by a factor 5) by keeping the catalyst removal yield quite high (around 99%) but the sample yield reported falls to 20% and even down to 13% for a further improvement of catalyst removal yield (99.8%). By comparison, the one-pot gas-phase treatment we propose appears as an original method with indisputable advantages of simplicity and low-time consuming. Moreover, the observed metal removal yield (up to 99%) is among the best yields reported coming along with an efficient elimination of carbon impurities from DWCNT samples. Amazingly, the quality of the purified DWCNTs is dramatically improved in this work since I_D/I_G is decreased by a factor of 15 after purification.

4. Conclusion

A one-pot gas-phase purification treatment was applied to a DWCNT sample. It simply consists in heating the CNT sample under a chlorine/oxygen atmosphere at around 1000 °C. An advantageous selective character of the combustion occurring during the purification stage favored the preparation of high-purity and high-quality DWCNTs. These latter contain very low content of both carbon and metal impurities. Interestingly, the removal of metal and carbon impurities comes with an improvement of DWCNT quality. We could show that the DWCNT surface is very clean without any functional group grafting. However, high amount of sample is consumed by such treatment. Compared to the existing methods, the overall yield of the treatment we propose considering several characteristics (including number of steps, metal removal yield, carbon impurities removal ability and sample consumption) is among the best purification approach already reported. Moreover, this method is versatile since by tuning the Cl_2/O_2 ratio, progressive catalyst and carbon impurity removal yields could be shown. We prove that our treatment is particularly suitable to treat CNTs of poor quality and containing high impurity content whereas numerous studies use rather good quality raw CNTs. Our developed method is particularly interesting to be applied to CNTs prepared by CVD which is the synthesis method adapted to large scale production and to CNTs dedicated to specific applications, such as magnetic or electrical properties.

Acknowledgments

The authors would like to thank Lionel Aranda for his help for TGA experiments and Pascal Franchetti for his valuable assistance for Raman spectroscopy. The authors would like to thank Dr. Gianrico Lamura for fruitful discussions. Angélica Vieira Bridi acknowledges CAPES Foundation for the scholarship no. 88888.076502/2013−00.

Appendix A. Supplementary data

Supplementary data related to this article can be found at http://dx.doi.org/10.1016/j.carbon.2016.09.033.

References

[1] M. Monthioux, E. Flahaut, C. Laurent, W. Escoffier, B. Raquet, W. Bacsa, et al., Properties of carbon nanotubes, in: B. Bhushan, et al. (Eds.), Handbook of Nanomaterials Properties, vol. 1, Springer-Verlag, Heidelberg, Germany, 2014, ISBN 978-3-642-31106-2, pp. 1−49.
[2] C. Shen, H. Alexandra, A. Brozen, Y.H. Wang, Double-walled carbon nanotubes: challenges and opportunities, Nanoscale 3 (2) (2011) 503−518.
[3] K.E. Moore, D.D. Tune, B.S. Flavel, Double-walled carbon nanotube processing, Adv. Mater. 27 (2015) 3105−3137.
[4] Y.A. Kim, K.S. Yang, H. Muramatsu, T. Hayashi, M. Endo, M. Terrones, et al., Double-walled carbon nanotubes: synthesis, structural characterization, and application, Carbon Lett. 15 (2) (2014) 77−88.
[5] E. Flahaut, R. Bacsa, A. Peigney, Ch Laurent, Gram-scale CCVD synthesis of double-walled carbon nanotubes, Chem. Commun. 12 (2003) 1442−1443.
[6] Q. Zhang, J.-Q. Huang, W.Z. Qian, Y.Y. Zhang, F. Wei, The road for nanomaterials industry: a review of carbon nanotube production, post-treatment, and bulk applications for composites and energy storage, Small 9 (8) (2013) 1237−1265.
[7] A.B. Makama, A. Salmiaton, N. Abdullah, S.Y. Thomas, T.S. Choong, E.B. Saion, Recent developments in purification of single wall carbon nanotubes, Sep. Sci. Technol. 49 (2014) 2797−2812.
[8] T. Bortolamiol, P. Lukanov, A.M. Galibert, B. Soula, P. Lonchambon, L. Datas, et al., Double-walled carbon nanotubes: quantitative purification assessment,

balance between purification and degradation and solution filling as an evidence of opening, Carbon 78 (2014) 79–90.
[9] H.G. Cho, S.W. Kim, H.J. Lim, C.H. Yun, H.S. Lee, C.R. Park, A simple and highly effective process for the purification of single-walled carbon nanotubes synthesized with arc-discharge, Carbon 47 (2009) 3544–3549.
[10] M.T. Martinez, M.A. Callejas, A.M. Benito, M. Cochet, T. Seeger, A. Anson, et al., Sensitivity of single wall carbon nanotubes to oxidative processing: structural modification, intercalation and functionalization, Carbon 41 (2003) 2247–2256.
[11] B. Vigolo, C. Hérold, J.-F. Marêché, J. Ghanbaja, M. Gulas, F. Le Normand, et al., A comprehensive scenario for commonly used purification procedures of arc-discharge as-produced single walled carbon nanotubes, Carbon 48 (2010) 949–963.
[12] P.-X. Hou, C. Liu, H.-M. Cheng, Purification of carbon nanotubes, Carbon 46 (2008) 2003–2025.
[13] L. Sheng, L. Shi, K. An, L. Yu, Y. Ando, X. Zhao, Effective and efficient purification of single-wall carbon nanotubes based on hydrogen treatment, Chem. Phys. Lett. 502 (2011) 101–106.
[14] Y. Li, H. Li, A. Petz, S. Kunsági-Maté, Reducing structural defects and improving homogeneity of nitric acid treated multi-walled carbon nanotubes, Carbon 93 (2015) 515–522.
[15] L. Cabana, X. Ke, D. Kepic, J. Oro-Solé, E. Tobias-Rossell, G. Van Tendeloo, G. Tobias, The role of steam treatment on the structure, purity and length distribution of multi-walled carbon nanotubes, Carbon 93 (2015) 1059–1067.
[16] J.L. Zimmerman, R. Kelley Bradley, C.B. Huffman, R.H. Hauge, J.L. Margrave, Gas-Phase Purification of single-wall carbon nanotubes, Chem. Mat. 12 (2000) 1361–1366.
[17] Y. Mackeyev, S. Bachilo, K.B. Hartman, L.J. Wilson, The purification of HiPco SWCNTs with liquid bromine at room temperature, Carbon 45 (2007) 1013–1017.
[18] Y.-Q. Xu, H. Peng, R.H. Hauge, R.E. Smalley, Controlled multistep purification of single-walled carbon nanotubes, Nano Lett. 5 (2005) 163–168.
[19] A.R. Harutyunyan, B.K. Prahan, J. Chang, G. Chen, P.C. Eklund, Purification of signe-wall carbon nantubes by selective microwave heating of catalyst particles, J. Phys. Chem. B 106 (2002) 8671–8675.
[20] V. Gomez, S. Irusta, O.B. Lawal, W. Adams, R.H. Hauge, C.W. Dunnill, A.R. Barron, Enhanced purification of carbon nanotubes by microwave and chlorine cleaning procedures, RSC Adv. 6 (2016) 11895–11902.
[21] K. MacKenzie, O. Dunens, A.T. Harris, A review of carbon nanotube purification by microwave assisted acid digestion, Sep. Purif. Technol. 66 (2009) 209–222.
[22] E.F. Antunes, V.G. de Resende, U.A. Mengui, J.B.M. Cunha, E.J. Corat, M. Massi, Analyses of residual iron in carbon nanotubes produced by camphor/ferrocene pyrolysis and purified by high temperature annealing, Appl. Surf. Sci. 257 (2011) 8038–8043.
[23] M. Yudasaka, T. Ichihashi, D. Kasuya, H. Kataura, S. Iijima, Structure changes of single-wall carbon nanotubes and single-wall carbon nanohorns caused by heat treatment, Carbon 41 (2005) 1273–1280.
[24] J. Barkauskas, I. Stankevičiene, A. Selskis, A novel purification method of carbon nanotubes by high-temperature treatment with tetrachloromethane, Sep. Purif. Technol. 71 (2010) 331–336.
[25] E.L.K. Chng, H.L. Poh, Z. Soferb, M. Pumera, Purification of carbon nanotubes by high temperature chlorine gas treatment, Phys. Chem. Chem. Phys. 15 (2013) 5615–5619.
[26] G. Mercier, C. Hérold, J.-F. Marêché, S. Cahen, J. Gleize, J. Ghanbaja, et al., Selective removal of metal impurities from single-walled carbon nanotube samples, New J. Chem. 37 (2013) 790–795.
[27] A. Desforges, G. Mercier, C. Hérold, J. Gleize, F. Le Normand, B. Vigolo, Improvement of carbon nanotube stability by high temperature oxygen/chlorine gas treatment, Carbon 76 (2014) 275–284.
[28] E. Remy, S. Cahen, B. Malaman, J. Ghanbaja, C. Bellouard, G. Medjahdi, et al., Quantitative investigation of mineral impurities of HiPco SWCNT samples: chemical mechanisms for purification and annealing treatments, Carbon 93 (2015) 933–944.
[29] C. Bellouard, G. Mercier, S. Cahen, J. Ghanbaja, G. Medjahdi, J. Gleize, G. Lamura, C. Hérold, B. Vigolo, Magnetism for understanding catalyst analysis of purified carbon Nanotubes, J. Magn. Magn. Mater. 411 (2016) 39–48.
[30] E. Flahaut, A. Peigney, W.S. Bacsa, R.R. Bacsa, C. Laurent, CCVD synthesis of carbon nanotubes from (Mg, Co, Mo)O catalysts: influence of the proportions of cobalt and molybdenum, J. Mater. Chem. 14 (2004) 646–653.
[31] A.S. Medvedev, N.V. Malochkina, Sublimation of molybdenum trioxide from exhausted catalysts employed for the purification of oil products, Russ. J. Non Ferr. Met. 48 (2) (2007) 114–117.
[32] N. Hultgren, L. Brewer, Gaseous molybdenum oxychloride, J. Phys. Chem. 60 (1956) 947–949.
[33] I.W. Chiang, B.E. Brinson, R.E. Smalley, J.L. Margrave, R.H. Hauge, Purification and characterization of single-wall carbon nanotubes, J. Phys. Chem. B 105 (2001) 1157–1161.
[34] R. Brukh, O. Sae-Khow, S. Mitra, Stabilizing single-walled carbon nanotubes by removal of residual metal catalysts, Chem. Phys. Lett. 459 (2008) 149–152.
[35] K.L. Strong, D.P. Anderson, K. Lafdi, J.N. Kuhn, Purification process for single-wall carbon nanotubes, Carbon 41 (2003) 1477–1488.
[36] Z. Shi, Y. Lian, F. Liao, X. Zhou, Z. Gu, Y. Zhang, et al., Purification of single-wall carbon nanotubes, Solid State Comm. 112 (1999) 35–37.
[37] B.I. Rosario-Castro, E.J. Contés, M. Lebrón-Colón, M.A. Meador, G. Sánchez-Pomales, C.R. Cabrera, Combined electron microscopy and spectroscopy characterization of as- received, acid purified, and oxidized HiPCO single-wall carbon nanotubes, Mater. Charact. 60 (2009) 1442–1453.
[38] A.C. Dillon, P.A. Parilla, J.L. Alleman, T. Gennett, K.M. Jones, M.J. Heben, Systematic inclusion of defects in pure carbon single-wall nanotubes and their effect on the Raman D-band, Chem. Phys. Lett. 401 (2005) 522–528.
[39] S. Osswald, E. Flahaut, H. Ye, Y. Gogotsi, Elimination of D-band in Raman spectra of double-wall carbon nanotubes by oxidation, Chem. Phys. Lett. 402 (2005) 422–427.
[40] E. Del Corro, J. Gonzales, M. Taravillo, E. Flahaut, V.G. Baonza, Raman spectra of double-wall nanotubes under extreme uniaxial pressures, Nano Lett. 045413 (8) (2008) 1–6.
[41] C. Lijie, Z. Zhenping, Y. Xiaoqin, L. Dongfang, Y. Huajun, S. Li, et al., Resonant Raman scattering of double wall carbon nanotubes prepared by chemical vapor deposition method, J. Appl. Phys. 94 (2003) 5715–5719.
[42] S. Osswald, E. Flahaut, Y. Gogotsi, In situ raman spectroscopy study of oxidation of double- and single-wall carbon nanotubes, Chem. Mater. 18 (6) (2006) 1525–1533.
[43] F.-H. Ko, C.-Y. Lee, C.-J. Ko, T.-C. Chu, Purification of multi-walled carbon nanotubes through microwave heating of nitric acid in a closed vessel, Carbon 43 (2005) 727–733.
[44] A.J. Clancy, E.R. White, H.H. Tay, H.C. Yau, M.S.P. Shaffer, Systematic comparison of conventional and reductive single-walled carbon nanotube purifications, Carbon 108 (2016) 423–432.
[45] J.M. Moon, K.H. An, Y.H. Lee, Y.S. Park, D.J. Bae, G.S. Park, High-yield purification process of single walled carbon nanotubes, J. Phys. Chem. B 105 (2001) 5677–5681.
[46] F. Li, H.M. Cheng, Y.T. Xing, P.H. Tan, G. Su, Purification of single-walled carbon nanotubes synthesized by the catalytic decomposition of hydrocarbons, Carbon 38 (2000) 2041–2045.